Temperature and pressure dependence of the elastic properties of $RbAg_4I_5$

L. J. Graham and R. Chang

Science Center, Rockwell International, Thousand Oaks, California 91360
(Received 17 February 1975)

An ultrasonic pulse superposition technique was used to measure the velocities of the three pure-mode waves which propagate along [110] in a single crystal of rubidium tetra-silver pentaiodide. The temperature was varied from 25 °C, through a phase transformation at −65 °C, and to a second phase transformation at −151 °C. There was a peak in the ultrasonic attenuation at the −65 °C transition for the longitudinal and one of the shear waves, and the attenuation and velocity of all of the waves were completely reversible upon cycling the temperature through this transition. The lower-temperature phase was generally several percent softer elastically than the room-temperature phase. Attempts to make measurements through the −151 °C transition were not successful. The pressure dependence of the wave velocities were determined at 25 °C. The adiabatic second-order elastic constants and their temperature and pressure derivatives at 25 °C which were determined from these measurements are as follows. The values of C_{ij} (10^{11} dyn/cm^2), C_{ij}^{-1} $(\partial C_{ij}/\partial T)$ (10^{-4} °K^{-1}), and $\partial C_{ij}/\partial P$ for C_{11} are 1.648 ± 0.002, -3.54 ± 0.12, and $+8.73\pm0.11$, respectively; for C_{12}, 0.934 ± 0.002, -3.73 ± 0.13, and $+6.29\pm0.11$, respectively; and for C_{44}, 0.4892 ± 0.0005, -4.17 ± 0.05, and $+0.884\pm0.015$, respectively. The Debye temperature of 90 °K and the thermal expansion coefficient of 0.566×10^{-4} °K^{-1} calculated from these values agree very well with values determined by other means.

PACS numbers: 62.20.D, 65.70., 64.70.K

I. INTRODUCTION

Rubidium tetra-silver pentaiodide is a member of the isostructural group of ionic compounds with the composition MAg_4I_5, where M includes Rb, K, and NH_4.[1–3] These compounds have the highest electrical conductivities of any known ionic solids, comparable to those of liquid electrolytes at room temperature. They are all thermodynamically unstable below room temperature, but can be retained for indefinite periods in a dry atmosphere well below room temperature. Of the three, the rubidium salt is the most stable and is of the greatest practical interest. During the five-year period, 1970 through 1974, over 50 research papers were published and 30 patents filed concerning this material. The present paper reports the only known measurements of its elastic properties, however. In this paper we report the results of measurements of the ultrasonic wave velocities and attenuation below room temperature, through a phase transformation at −65 °C, and to a second phase transformation at −151 °C. Also reported are the pressure dependences of the ultrasonic wave velocities at 25 °C. From these measurements the second-order adiabatic elastic constants and their temperature and pressure derivatives at 25 °C were calculated. Other parameters such as the Debye temperature, thermal expansion coefficient, and equivalent isotropic elastic moduli which can be calculated from the single-crystal elastic constants are also reported.

II. EXPERIMENTAL PROCEDURE

The elastic constants of $RbAg_4I_5$ were measured using a sensitive phase-comparison ultrasonic pulse-echo method[4] on a single crystal grown using the Czochralski technique.[5] At room temperature this material has a cubic crystal structure[6] and thus its elastic properties are described by three independent elastic constants C_{11}, C_{12}, and C_{44}. These can be determined conveniently by measuring the three independent ultrasonic wave velocities which can propagate along a [110] direction in the crystal and which provide three combinations of the elastic constants as the product of the velocity squared times the density. These three velocities were measured as a function of temperature at 1 atm pressure and as a function of pressure at 25 °C. During the temperature runs, the ultrasonic attenuation was also monitored.

The size of the single crystal used in this study was $\frac{1}{2}\times\frac{1}{2}\times\frac{1}{8}$ in., oriented so the $\frac{1}{8}$-in. direction through the crystal was the [110] wave propagation direction. The two $\frac{1}{2}$-in. square {110} faces were polished optically flat and parallel. The ultrasonic measurements were made using $\frac{1}{8}$-in.-diam 16-MHz quartz transducers bonded to the [110] face with Salol between room-temperature and about −45 °C, and with 2.5×10^6-centistoke Dow Corning 200 silicone fluid below −45 °C. The x-ray density of $\rho=5.384$ g/cm^3 determined by Geller[6] was used in calculating the elastic constants.

III. PHASE TRANSFORMATIONS IN $RbAg_4I_5$

$RbAg_4I_5$ undergoes two phase transformations below room temperature, at about −65 °C and −151 °C. Upon cooling a single crystal below −65 °C it becomes optically birefringent; this transition is reversible with no hysteresis.[6] At this temperature there is only a slight change in slope of the temperature dependence of electrical conductivity,[1] and the x-ray powder pattern at −100 °C shows line broadening and at least one split line.[6] Although the crystal structure of this intermediate phase has not been determined it cannot be cubic, and therefore more than three elastic constants are required to describe its elastic behavior. However, the

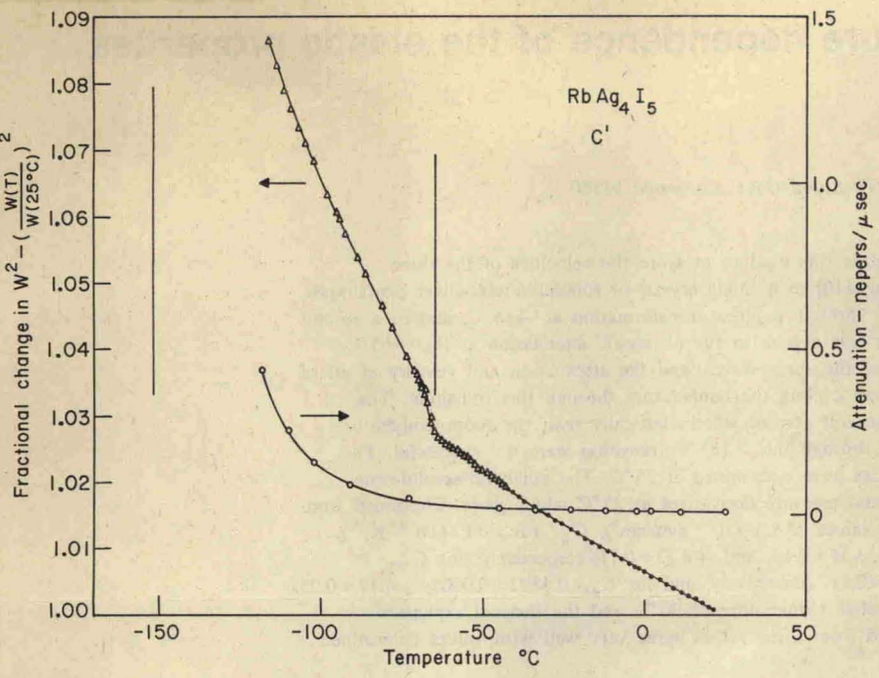

FIG. 1. Data for the shear mode which determines the C' elastic constant. Phase transformations occur at −65 and −151 °C.

ultrasonic pulse-echo patterns observed below the −65 °C transition showed no detectable distortion. This can only be explained if the wave propagation direction happened to be a pure-mode direction in the noncubic structure, or if the deformations associated with the structure change were small enough so that the wave propagation characteristics of the crystal were not greatly affected. There is, therefore, some justification in analyzing and presenting the ultrasonic data for the noncubic phase as if it were pseudocubic, although it should be kept in mind that this analysis is not rigorously valid.

At the −151 °C transition there is a step decrease in the electrical conductivity of two orders of magnitude which is reversible upon reheating.[1] Also, new lines appear in the powder x-ray diffraction pattern for the low-temperature phase.[6] These observations indicate a substantial change in crystal structure at this transition. An attempt to make ultrasonic measurements through this transition was unsuccessful.

IV. RESULTS

Figure 1 shows the results for the shear wave which determines the elastic constant C' which is $\frac{1}{2}(C_{11}-C_{12})$ in terms of the elastic constants referred to the cubic coordinate system. On the left abscissa is plotted the fractional change in the square of the natural wave velocity, W. This is the same as the fractional change in C', except that the correction for thermal expansion has not been made. The effect of this correction would be to make the slope of this curve more negative by a few percent, but the data to make this correction are not available. The two vertical lines indicate the temperatures of the two phase transitions determined from the centers of two spikes in the specific-heat—vs—temperature data to be −64.3 and −151.4 °C.[7] The data points for the elastic modulus curve around the −65 °C transition are from several runs while both increasing and decreasing the temperature, and illustrate that the elastic behavior through this transition is reversible with less than 0.2 °C hysteresis if any.

On the right abscissa is the ultrasonic attenuation in Np/μsec. The attenuation is seen to be very flat through the transition region for this wave mode, then it increases sharply well above the −151 °C transition. When the attenuation reaches a value of about 0.5 Np/μsec, each successive echo in the pulse-echo pattern is down by about 17 dB and the wave velocity measurement can no longer be made. When the attenuation reached that value, this run was terminated.

The other shear mode measured gives the elastic constant C_{44} directly. In contrast to the C' shear, the C_{44} shear exhibits a large ultrasonic attenuation peak at −65 °C as is shown in Fig. 2. The peak in attenuation is asymmetric with respect to the transition temperature, the slope of the low-temperature side being much steeper. Again, this behavior was apparently completely reversible with no hysteresis. It is also seen that the elastic modulus C_{44} of the cubic phase anticipates the phase change 40—50 °C above the transition temperature, its value falling rapidly as the temperature is decreased. By extrapolating the elastic constants of the two phases to the transition temperature it is seen that there is a 4—5% difference, whereas the C' constant changed by less than 1%.

The results for the longitudinal wave mode are shown in Fig. 3. This mode determined the elastic constant C_L, which is $\frac{1}{2}(C_{11}+C_{12}+2C_{44})$ in terms of elastic constants referred to the cubic coordinate system. For this mode there is again a strong attenuation peak at the −65 °C transition. The asymmetry of this peak can be seen more readily since it was possible to make measurements over the top of the peak. The

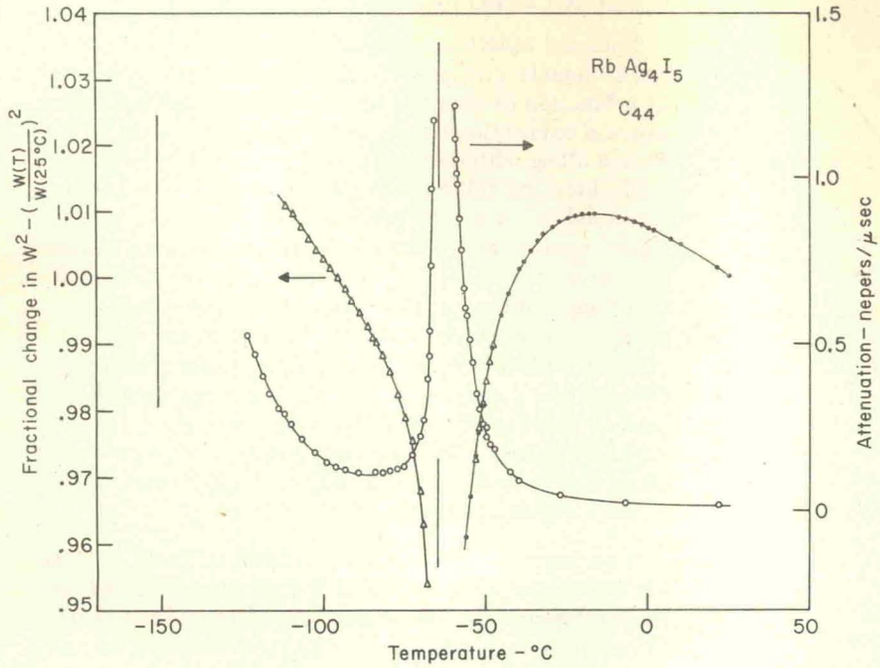

FIG. 2. Data for the shear mode which determines the C_{44} elastic constant. Phase transformations occur at −65 and −151 °C.

peak position determined from these data was −64.9 ± 0.1 °C, somewhat lower than the transition temperature determined calorimetrically.[7] The elastic constant C_L above the −65 °C transition anticipates this transition and starts to decrease in value 40–50 °C above the transition temperature as did C_{44}. The change in value across the transition is less, however, being only about 3%.

At temperatures below −65 °C, the attenuation returned to relatively low values for this mode. An attempt was therefore made to follow the attenuation through the −151 °C transition. However, upon going through this transition the single crystal cracked in several places, and the acoustic bond between the quartz transducer and the sample broke. Therefore, no acoustic data below the transition temperature were obtained. However, the attenuation data approaching this temperature show that there is no ultrasonic attenuation peak for this wave mode at the low temperature.

The dependence of the three wave velocities on hydrostatic pressure for the cubic phase at 25 °C were also measured. These data are shown in Fig. 4. Here are plotted the change in the natural wave velocities, W, normalized to their zero pressure value versus pressure for the three ultrasonic waves. The slopes of these plots at $P=0$ are related to certain combinations of the third-order elastic constants of the material.[8] The open symbols on these plots signify data taken

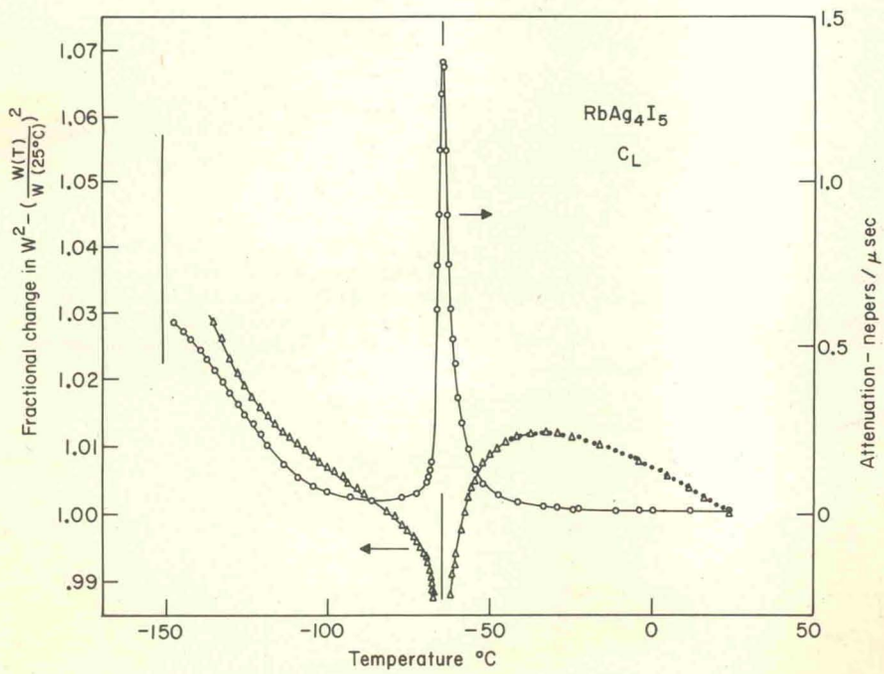

FIG. 3. Data for the longitudinal mode which determines the C_L elastic constant. Phase transformations occur at −65 and −151 °C.

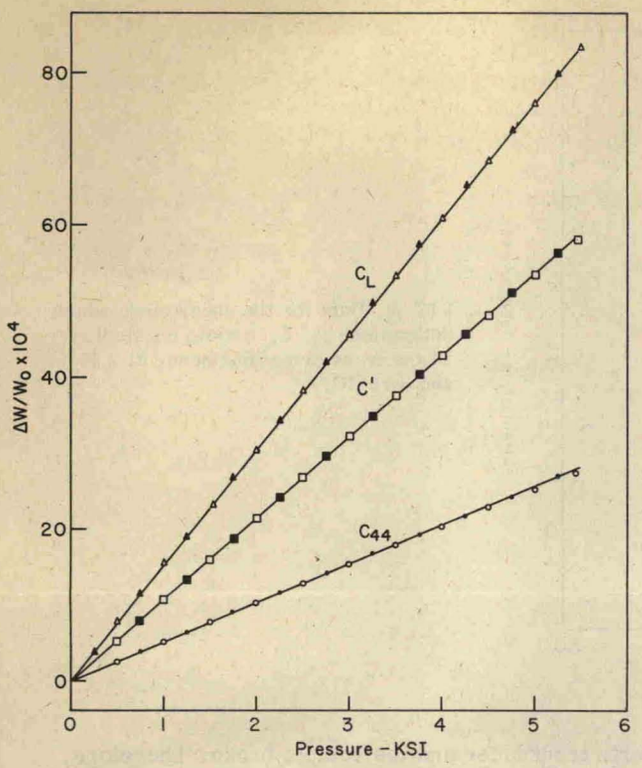

FIG. 4. Data for the pressure dependence at 25 °C of the natural wave velocities for the three wave modes measured.

while the pressure was increased and the closed symbols while the pressure was decreased. At each pressure step temperature equilibrium was established in the sample by waiting about 15 min before taking the data. Temperature corrections back to 25 °C were then made since the sample heated up 1—2 °C while increasing the pressure to its maximum value, and cooled while decreasing the pressure.

V. CALCULATED RESULTS

Since the elastic constants C_L equals $\frac{1}{2}(C_{11}+C_{12}+2C_{44})$ and C' equals $\frac{1}{2}(C_{11}-C_{12})$, we can also plot C_{11} and C_{12} as a function of temperature (except for the thermal expansion correction as before). These are shown in Fig. 5 along with the bulk modulus K, which is $\frac{1}{3}(C_{11}+2C_{12})$ for the cubic phase. As closely as could be determined by taking the appropriate differences in the experimental data, all three of these constants behave normally with temperature right to the −65 °C transition temperature. At that point they make a step change in value of from 1—3% similar to the way C' changed with temperature in Fig. 1, except these changes are negative. In fact all of the constants except C' decrease going through the transition, indicating that the lower-temperature phase may be generally about 2—3% softer than the higher-temperature phase at the same temperature.

A summary of all the data is shown in Table I. Here are shown the 25 °C values of the elastic constants and their temperature and pressure derivations based on the natural wave velocities. The first three items in each column were directly determined experimentally, and the other entries were calculated from them. The uncertainties in the directly measured quantities are conservative estimates based on repeated measurements on the same crystal. In addition, a second crystal in a [100] orientation was available for a short time, and values of C_{11} and C_{44} determined for this crystal agreed within 0.1% of the values quoted in Table I. The temperature and pressure derivatives of these elastic constants were not measured for the [100]-oriented crystal, however.

The true temperature and pressure derivatives of the adiabatic elastic constants are related to the derivatives based on the natural wave velocities by the relations[8]

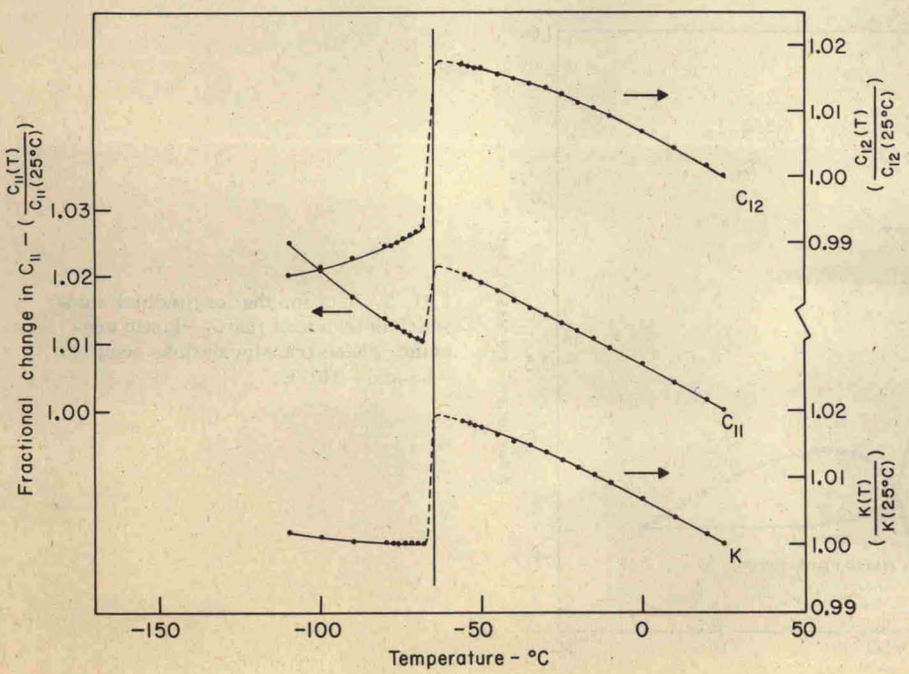

FIG. 5. Temperature dependence of the elastic constants C_{11} and C_{12} and the bulk modulus K obtained from the appropriate sums of the data of Figs. 1—3. The thermal expansion correction has not been applied to these data.

TABLE I. Adiabatic elastic constants of $RbAg_4I_5$ at 25 °C and their temperature and pressure derivatives based on the measured natural wave velocities. The first three entries in each column were directly determined experimentally, and the other entries were calculated from them.

	C_{ij} (10^{11} dyn/cm^2)	$\frac{1}{\rho_0 W^2}\frac{\partial(\rho_0 W^2}{\partial T}$ (10^{-4} °K^{-1})	$\frac{\partial(\rho_0 W^2)}{\partial P}$
C_L	1.780 ± 0.002	−3.19 ± 0.10	+7.85 ± 0.08
C'	0.3568 ± 0.0003	−2.72 ± 0.02	+1.115 ± 0.010
C_{44}	0.4892 ± 0.0005	−3.60 ± 0.05	+0.734 ± 0.015
C_{11}	1.648 ± 0.002	−2.97 ± 0.12	+8.23 ± 0.11
C_{12}	0.934 ± 0.002	−3.16 ± 0.13	+6.00 ± 0.11
K	1.172 ± 0.003	−3.07 ± 0.13	+6.74 ± 0.11

$$\frac{1}{C}\left(\frac{\partial C}{\partial T}\right)_P = \frac{1}{\rho_0 W^2}\left(\frac{\partial(\rho_0 W^2)}{\partial T}\right)_P - \alpha, \tag{1}$$

$$\left(\frac{\partial C}{\partial P}\right)_{T,P=0} = \left(\frac{\partial(\rho_0 W^2)}{\partial P}\right)_{T,P=0} + \frac{C}{3K^T}, \tag{2}$$

where C is the adiabatic elastic modulus in question, α is the linear thermal expansion coefficient, and K^T is the isothermal bulk modulus. This can be obtained from the relation[9]

$$\frac{K^S}{K^T} = 1 + \frac{9\alpha^2 K^S T}{\rho C_p}. \tag{3}$$

An approximate value of $\alpha = 0.57\times10^{-4}$ °K^{-1} was obtained from lattice parameter measurements at 25 °C and −50 °C.[10] Using a value of the heat capacity $C_p = 0.0593$ cal/g °K,[7] $K^S/K^T = 1.077$, and $K^T = 1.089\times10^{11}$ dyn/cm^2. These values of α and K^T can be used in Eqs. (1) and (2) to convert the values of the temperature and pressure derivatives shown in Table I to the true values with very little error. These are shown in Table II.

There are several bulk property values that can be calculated from the single-crystal elastic constants. The elastic properties of an isotropic polycrystalline solid of the same material are often required since technological use of the polycrystalline material is more common than of the single crystal. An approximation to the polycrystalline values can be obtained from the single-crystal elastic constants using the Voigt-Reuss-Hill[11] or the Hashin-Shtrikman[12] methods. For $RbAg_4I_5$ both methods yield the same values for Young's modulus, shear modulus, and Poisson's ratio which are $E = 1.155\times10^{11}$ dyn/cm^2, $G = 0.432\times10^{11}$ dyn/cm^2, and $\nu = 0.336$ at 25 °C.

Using these values for the average bulk elastic properties, the Debye characteristic temperature can be calculated.[13] This was in fact done at three temperatures, 25, −68, and −110 °C which resulted in the values for θ_D of 90.8, 90.3, and 92.5 °K, respectively. These values should be within a few percent of the value determined calorimetrically if the elastic behavior of the low-temperature phase is not too different from that of the high-temperature phases. The specific-heat data result in a Debye temperature of 92 °K,[7] which suggests that this is indeed the case.

Another bulk property value which can be calculated from the single-crystal elastic constants and their pressure derivatives is the Grüneisen parameter, γ. The thermal expansion coefficient at 25 °C can be obtained from this value through the relation

$$\alpha = \rho C_p \gamma / 3K^S \tag{4}$$

for comparison with the approximate value used in the previous calculations. An estimate of its temperature dependence could also be obtained from the temperature dependence of C_p,[7] since the other parameters in this relation are relatively insensitive to temperature. This could be used with the data of Figs. 1–3 to obtain a better estimate of the temperature dependence of the single-crystal elastic constants, if this was desired.

In the Debye model, a Grüneisen parameter can be expressed in terms of the second- and third-order elastic constants for each of the standing wave modes of the elastic continuum. The Grüneisen parameter which describes the average bulk properties can be obtained by the appropriate averaging over all possible wave modes. In lieu of this for a crystal with cubic symmetry, an approximation can be made by averaging over only the 39 pure-wave modes which can propagate in the directions of the cube edges and the face and body diagonals. The expressions for the mode γ's associated with each of these waves have been derived previously.[14] Instead of taking the sum of all of these mode γ's, we sum the ones associated with longitudinal and shear modes separately resulting in the equations

$$\gamma_L = -\frac{1}{13}\left(\frac{3C_{11}+2C_{12}+C_1}{2C_{11}} + \frac{2(5C_{11}+10C_{12}+8C_{44}+3C_1+4C_2-4C_3)}{3(C_{11}+2C_{12}+4C_{44})} + \frac{2(2C_{11}+3C_{12}+2C_{44}+C_1+C_2-C_3)}{C_{11}+C_{12}+2C_{44}}\right), \tag{5}$$

$$\gamma_S = -\frac{1}{26}\left(\frac{2(C_{11}+2C_{12}+2C_{44}+C_2)}{C_{44}} + \frac{4(5C_{11}+4C_{12}+2C_{44}+C_2+2C_3)}{3(C_{11}-C_{12}+C_{44})} + \frac{2(2C_{11}+C_{12}+C_3)}{C_{11}-C_{12}}\right), \tag{6}$$

TABLE II. Temperature and pressure derivatives of the adiabatic second-order elastic constants of $RbAg_4I_5$ at 25 °C and 1 atm pressure.

	$\frac{1}{C}\left(\frac{\partial C}{\partial T}\right)_P$ (10^{-4} °K^{-1})	$\left(\frac{\partial C}{\partial P}\right)_{T,P=0}$
C_{11}	−3.54 ± 0.12	+8.73 ± 0.11
C_{12}	−3.73 ± 0.13	+6.29 ± 0.11
C_{44}	−4.17 ± 0.05	+0.884 ± 0.015
C_L	−3.76 ± 0.10	+8.40 ± 0.08
C'	−3.29 ± 0.02	+1.224 ± 0.010
K	−3.64 ± 0.13	+7.10 ± 0.11

where the C_{ij} are the adiabatic second-order elastic constants, and the C_i are the combinations of third-order elastic constants $C_1 = C_{111} + 2C_{112}$, $C_2 = C_{144} + 2C_{166}$, and $C_3 = \frac{1}{2}(C_{111} - C_{123})$. These combinations of the third-order elastic constants are determined uniquely by the hydrostatic pressure derivatives of the second-order constants shown in Table I.[8] Their values in the units of 10^{12} dyn/cm^2 are $C_1 = -3.30$, $C_2 = -0.656$, and $C_3 = -0.752$. For temperatures greater than θ_D,

$$\gamma = \tfrac{1}{3}(\gamma_L + 2\gamma_S). \tag{7}$$

Evaluating Eqs. (5)–(7) results in $\gamma = 1.49$, and using this value in Eq. (4) gives $\alpha = 0.566 \times 10^{-4}\,^{\circ}\mathrm{K}^{-1}$ which agrees with the value $0.57 \times 10^{-4}\,^{\circ}\mathrm{K}^{-1}$ determined from lattice parameter measurements. This agreement validates the calculated temperature and pressure derivatives of the elastic constants shown in Table II.

[1] B.B. Owens and G.R. Argue, Science **157**, 308 (1967).
[2] J.N. Bradley and P.D. Greene, Trans. Faraday Soc. **62**, 2069 (1966).
[3] J.N. Bradley and P.D. Greene, Trans. Faraday Soc. **63**, 424 (1967).
[4] L.J. Graham, H. Nadler, and Roger Chang, J. Appl. Phys. **39**, 3025 (1968).
[5] L.D. Fullmer and M.A. Hiller, J. Cryst. Growth **5**, 395 (1969).
[6] S. Geller, Science **157**, 310 (1967).
[7] W.V. Johnston, H. Wiedersich, and G.W. Lindberg, J. Chem. Phys. **51**, 3739 (1969).
[8] R.N. Thurston and K. Brugger, Phys. Rev. **133**, A1604 (1964).
[9] D.H. Chung, J. Appl. Phys. **38**, 5104 (1967).
[10] W.V. Johnston (private communication).
[11] R. Hill, Proc. Phys. Soc. Lond. A **65**, 349 (1952).
[12] Z. Hashin and S. Shtrikman, J. Mech. Phys. Solids **10**, 335 (1962); **10**, 343 (1962).
[13] O.L. Anderson, J. Phys. Chem. Solids **24**, 909 (1963).
[14] W.P. Mason and T.B. Bateman, J. Acoust. Soc. Am. **36**, 644 (1964).